


Observation of Traveling Breathers and Their Scattering in a Two-Fluid System

Yifeng Mao^{1,*}, Sathyanarayanan Chandramouli², Wenqian Xu¹ and Mark A. Hoefer¹

¹*Department of Applied Mathematics, University of Colorado, Boulder, Colorado 80309, USA*

²*Department of Mathematics, Florida State University, Tallahassee, Florida 32306, USA*

 (Received 21 February 2023; revised 23 May 2023; accepted 30 August 2023; published 3 October 2023)

The observation of traveling breathers (TBs) with large-amplitude oscillatory tails realizes an almost 50-year-old theoretical prediction [E. A. Kuznetsov and A. V. Mikhailov, *Stability of stationary waves in nonlinear weakly dispersive media*, *Zh. Eksp. Teor. Fiz.* **67**, 1717 (1974) [*Sov. Phys. JETP* **40**, 855 (1975)]] and generalizes the notion of a breather. Two strongly nonlinear TB families are created in a core-annular flow by interacting a soliton and a nonlinear periodic (cnoidal) carrier. Bright and dark TBs are observed to move faster or slower, respectively, than the carrier while imparting a phase shift. Agreement with model equations is achieved. Scattering of the TBs is observed to be physically elastic. The observed TBs generalize to many continuum and discrete systems.

DOI: [10.1103/PhysRevLett.131.147201](https://doi.org/10.1103/PhysRevLett.131.147201)

Fifty years ago, special, localized two-soliton bound state solutions of the sine-Gordon equation were called “breathers” because they incorporate two timescales: one associated with propagation and the other associated with internal oscillation [1]. The term breather has since been generalized to solutions of other completely integrable systems such as the modified Korteweg–de Vries (KdV) and the focusing nonlinear Schrödinger equations [2]. However, the strict notion of localized breather solutions appears to be limited to integrable equations. Numerical simulations [3–5] and mathematical analysis [6,7] demonstrate that breathers in some nonintegrable equations necessarily display small oscillatory tails. Consequently, they have been referred to as quasibreathers [2] or nonlocal solitary waves [8], although, in some instances, these oscillatory tails may be vanishingly small [9].

Small amplitude breathers can be approximated by bright soliton solutions of the focusing nonlinear Schrödinger equation. Consequently, breathers have been observed in many situations such as water waves [10,11], internal waves [12], nonlinear optical [13–15] and matter [16,17] waves, rogue waves in these systems [18–22], magnetic materials [23], and discrete systems [24,25].

Breathers with nonvanishing oscillatory tails have been studied extensively in lattice systems where they are commonly referred to as traveling intrinsic localized modes or “traveling breathers” [24,26,27] with experimental observations of their existence in [28,29]. In the continuum setting, special solutions, originally called solitary dislocations, were derived for the KdV equation as the nonlinear superposition of a soliton and a cnoidal traveling periodic wave in the seminal work of Kuznetsov and Mikhailov [30]. This was achieved using inverse scattering theory by introducing a discrete eigenvalue, representing the soliton, in either the finite or semi-infinite gap of the cnoidal wave

spectrum for the Schrödinger operator associated with KdV. This solution is a traveling breather with large amplitude oscillatory tails that can be of either elevation (bright) or depression (dark) type depending on the eigenvalue location in the semi-infinite gap or finite gap, respectively. The cnoidal wave can also be considered a soliton lattice and so this traveling breather can be viewed as a soliton-soliton lattice interaction, generalizing the localized two-soliton bound state breathers in, e.g., sine-Gordon and modified KdV [2]. The scattering theory for KdV traveling breathers indicates that they interact with each other elastically, experiencing only a spatial shift [30]. Despite much ensuing analysis [31–40] and corresponding physical interest, the observation and scattering of strongly nonlinear traveling breathers in continuum mechanics is lacking.

In this Letter, we create and scatter strongly nonlinear elevation wave or bright (BB) and depression wave or dark (DB) traveling breathers at the interface between two viscous fluids by the overtaking interaction of a carrier wave with a soliton or vice versa. The traveling breather oscillatory tails—the carrier background—are large amplitude. The results experimentally prove that this class of breathers can be interpreted as a nonlinear superposition between a soliton and a cnoidal-like wave, realizing the spectral interpretation of a traveling breather from inverse scattering theory developed almost 50 years ago [30,40].

Additionally, we measure traveling breather properties during free propagation and scattering, finding that they retain their solitonic character, i.e., interactions are physically elastic. Unimodal and bimodal geometries of internal oscillation are observed. Qualitative or quantitative features of individual traveling breathers and their scattering agree with predictions from KdV traveling breather theory or numerical simulations of a viscous two-fluid nonlinear

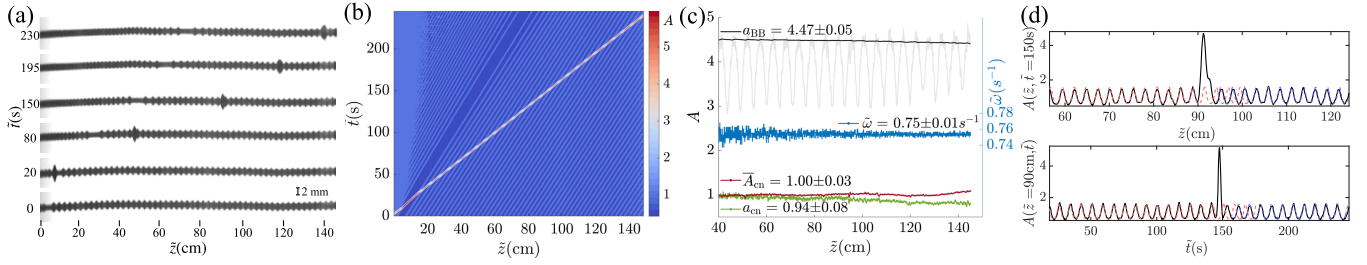


FIG. 1. Bright traveling breather (BB) in a viscous fluid conduit formed from a soliton overtaking a cnoidal-like periodic traveling wave. (a) 90° clockwise rotated time lapse. (b) Space-time contour of the cross-sectional area. (c) Background cnoidal-like wave and BB measurements at different heights. (d) Spatial and temporal profiles (black solid) and the cnoidal-like wave solution of the conduit equation (1) corresponding to measured parameters (dashed).

model, respectively. Increasing traveling breather speeds imply decreasing (BB) or increasing (DB) carrier phase shifts. Slower (faster) traveling breathers exhibit a negative (positive) spatial shift postinteraction. The observation of traveling breathers in this model continuum system and their characterization are relevant to the physics of nonlinear dispersive media more broadly.

The experiments are conducted in a tall acrylic column of 5 cm × 5 cm × 180 cm, described in [41]. The column consists of a pressure-driven viscous core fluid with a free interface to a miscible, heavier viscous reservoir fluid with a small core-to-reservoir fluid viscosity ratio. We precisely control the injection of the buoyant, interior fluid in the low Reynolds number regime, which is convectively unstable [42,43], so that straight conduits are established with constant injection. Time-varying injection results in a conduit that exhibits an azimuthally symmetric interface with cross-sectional area $A(z, t)$, where $z > 0$ is the vertical spatial coordinate in the camera view that is slightly above the injection site. We identify $t = 0$ as the time at the initiation of interfacial imaging. At the injection site, the cross-sectional area satisfies the Hagen-Poiseuille flow law $Q \propto A^2$ so it can be precisely controlled by temporally varying the injection rate Q [44,45].

Viscous core-annular interfacial waves are modeled by the strongly nonlinear conduit equation expressing mass conservation [45,46]

$$A_t + (A^2)_z - (A^2(A^{-1}A_t)_z)_z = 0, \quad (1)$$

given in nondimensional form where $z = \tilde{z}/L$, $t = \tilde{t}/T$, $A = \tilde{A}/A_0$ for dimensional quantities \tilde{z} , \tilde{t} , \tilde{A} , and L , T , A_0 are the fitted vertical length, time, and cross-sectional area, respectively, obtained from separate measurements of linear dispersive waves on the background injection rate $Q_0 \propto A_0^2$ [47]. The conduit equation (1) and variants of it are models of magma flow [49] and channelized water flow in glaciers [50]. The conduit equation is apparently not integrable and can be reduced to the KdV equation in the long-wavelength and small-amplitude regime [47,51]. Cnoidal-like waves in the form $A(z, t) = g(\theta)$,

$\theta = kz - \omega t$, $g(\theta + 2\pi) = g(\theta)$ and solitons are generated by evaluating numerically computed traveling wave solutions of the conduit equation [52] at the injection site, which determines the injection rate time series $Q(t) \propto g(-\omega t)^2$. The characterization and reliable generation of soliton and cnoidal-like waves have, individually, been reported in [41,45,53].

Figure 1 displays the spatiotemporal evolution of a soliton overtaking a cnoidal-like wave. At $t = 0$, we have prepared the conduit as a nonlinear cnoidal-like wave (the “carrier”) that abruptly terminates at the injection site to a constant flow rate for $t > 0$. The carrier propagates upward for positive z and experiences a modulation region as it transitions from periodic to a constant background [Fig. 1(a) for $t > 20$ s, Fig. 1(b)] [47]. This modulated region consists of a dispersive shock wave [54], a constant region whose value A_{\min} coincides with the minimum of the adjacent carrier, and a carrier modulation [54,55]. The averaged carrier’s amplitude (a_{cn}), mean (\bar{A}_{cn}), and dimensional angular frequency ($\tilde{\omega} = \omega/T$) are reported in Fig. 1(c). The measured angular wave number ($\tilde{k} = k/L$) is $\tilde{k} = 2.35 \pm 0.01 \text{ cm}^{-1}$. After terminating the carrier, a large-amplitude soliton is injected, which is transmitted through the dispersive shock wave [56] and the constant region A_{\min} . Because the soliton speed on the constant region A_{\min} exceeds the carrier’s phase speed ($\tilde{v}_{\text{ph}} = \tilde{\omega}/\tilde{k}$), the soliton overtakes the carrier and forms a new coherent structure. The amplitude of the coherent structure extracted from experiment [$a_{\text{BB}}(z) = \max_t A(z, t) - A_{\min}$] oscillates with propagation. In Fig. 1(c), we plot $a_{\text{BB}}(z)$, its envelope, and the carrier’s properties extracted from each spatial slice of Fig. 1(b) to characterize propagation up the conduit. The amplitude, mean, and frequency of the carrier and the coherent structure’s amplitude envelope exhibit small fluctuations with height z . We conclude that the coherent structure is a BB consisting of the nonlinear superposition of a soliton and a cnoidal-like wave.

Next, we extract the BB’s maximum value for $\tilde{z} \gtrsim 40$ cm in Fig. 1(b) that follows a zigzag path with constant speed regularly interspersed between regions of rapid acceleration and deceleration. The BB speed across the entire zigzag

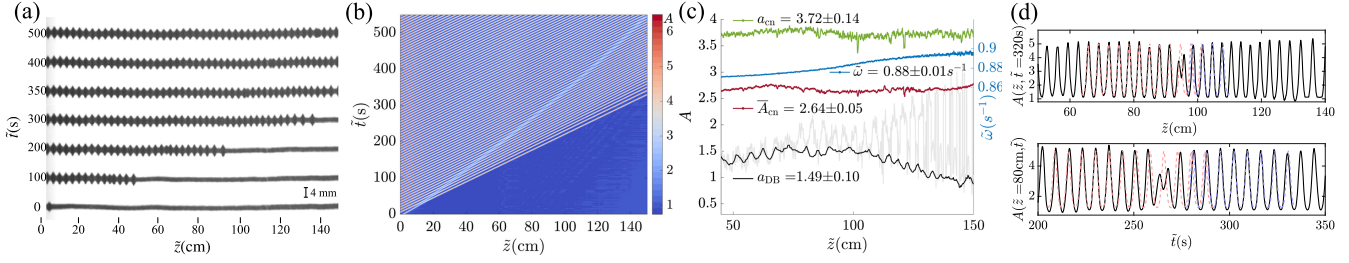


FIG. 2. Absorption of a solitary wave by a larger-mean, larger-amplitude cnoidal-like periodic traveling wave resulting in a dark traveling breather. (a) 90° clockwise rotated time-lapse images. (b) Space-time contour. (c) Background cnoidal-like wave and DB measurements. (d) Spatial and temporal profiles (black solid) and the cnoidal-like wave solution of (1) corresponding to measured parameters (dashed).

path is $\tilde{v}_{\text{BB}} = 0.63 \pm 0.01$ cm/s [47], which exceeds the measured carrier phase speed $\tilde{v}_{\text{ph}} = 0.319 \pm 0.005$ cm/s. This is consistent with KdV BB solutions [30,39]. A more thorough analysis of the BB trajectory [47] shows that it can also be viewed as a soliton undergoing a sequence of phase shifts while interacting with a soliton lattice that composes the cnoidal-like wave [30,57].

In Fig. 1(d), we extract experimental time and spatial slices of $A(z, t)$. The measured BB's phase shift in space and time $\Delta\theta \in (-\pi, \pi]$ is defined as the difference between the left and right carrier phases. We find that $\Delta\theta_{\text{BB}z} = 0.72\pi$ in space and $\Delta\theta_{\text{BB}t} = 0.75\pi$ in time are comparable, as expected. This BB with a positive phase shift is consistent with large-amplitude BB solutions of the KdV equation [39].

To generate a DB, the cnoidal-like carrier is set to overtake the soliton. So that the carrier fully absorbs the soliton, it is essential to increase the mean flow rate of the carrier relative to the soliton. This approach is reported in Figs. 2(a) and 2(b) where, now, soliton-cnoidal-like wave interaction results in a depression defect, a DB. For each fixed z , we define the DB amplitude $a_{\text{DB}}(z)$ as the difference between the maximum of the carrier and the minimum of the DB upper envelope. The measured averaged carrier parameters are given in Fig. 2(c) and $\tilde{k} = 1.95 \pm 0.03$ cm $^{-1}$. In contrast to the BB case, the carrier frequency shown in Fig. 2(c) increases up the conduit. The carrier with a larger mean than the soliton leads to more carrier fluctuations than in the BB case. Near the top of the conduit, we observe a 5% increase in the carrier mean and a corresponding change in other DB properties. Generally, the injected interior fluid is suspended at the top after rising through the exterior fluid. We attribute DB modulations for $\tilde{z} > 110$ cm to the slow diffusion of interior fluid from the top, which lowers the exterior fluid's density ρ_e . The observed 5% mean increase can be explained by a correspondingly small 2.5% decrease in the exterior to interior density difference via the Hagen-Poiseuille law in which $\bar{A} \propto (\rho_e - \rho_i)^{-1/2}$ [46]. Note that a similar mean increase near the top is observed for the BB in Fig. 1(c). Despite this, propagation of the DB is robust over

a large portion of the conduit $\tilde{z} \in [80, 110]$ cm where carrier and DB fluctuations are modest.

The measured DB speed is $\tilde{v}_{\text{DB}} = 0.27 \pm 0.01$ cm/s over $\tilde{z} \in [80, 110]$ cm while the carrier phase speed is larger $\tilde{v}_{\text{ph}} = 0.45 \pm 0.01$ cm/s, a characteristic feature of KdV DBs [30,39]. Figure 2(d) shows spatial, temporal slices and the determination of the carrier phase shift. The phase shifts are $\Delta\theta_{\text{DB}z} = 0.24\pi$ in space and $\Delta\theta_{\text{DB}t} = 0.25\pi$ in time.

While qualitative features of observed BBs and DBs agree with KdV theory, KdV is a quantitative model only for small amplitude, $a \ll 1$, long waves, $k \ll 1$, subject to the dominant balance $a \sim k^2$, where a and k are the nondimensional amplitude and wave number of the carrier, respectively. Since $a \gtrsim 1$ and $k \approx 0.4$ in our experiments, the dominant balance and smallness conditions are not satisfied. Consequently, we perform numerical simulations of the strongly nonlinear conduit equation (1) with periodic boundary conditions and an initial condition extracted from the time sliced experimental sections in Figs. 1(d) and 2(d). Figure 3 depicts a comparison of the simulations, experiment, and a KdV traveling breather with fitted carrier and phase shift in the comoving reference frame [47]. In Fig. 3(a), an oscillation period of the BB $[\tilde{T}_{\text{BB}} = 2\pi/(\tilde{v}_{\text{BB}}\tilde{k} - \tilde{\omega})] \approx 9$ s] is shown in the top four panels with the much smaller than observation KdV BB solution. Viewed as a soliton-soliton lattice interaction, the BB exhibits the unimodal interaction geometry according to the Lax categories of two-soliton interactions

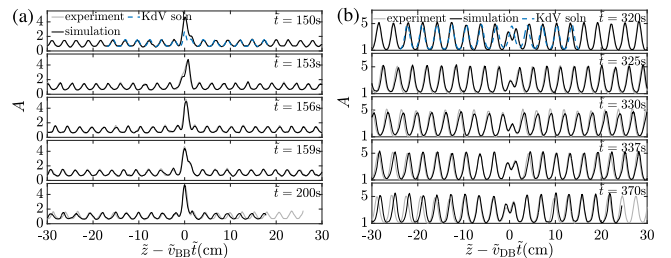


FIG. 3. Experiment (light gray) compared with simulation of the conduit equation (1) (black) with initial conditions from experiment, and the KdV traveling breather solution (blue). (a) BB from Fig. 1(d). (b) DB from Fig. 2(d). The top four panels in (a),(b) present the evolution over one period.

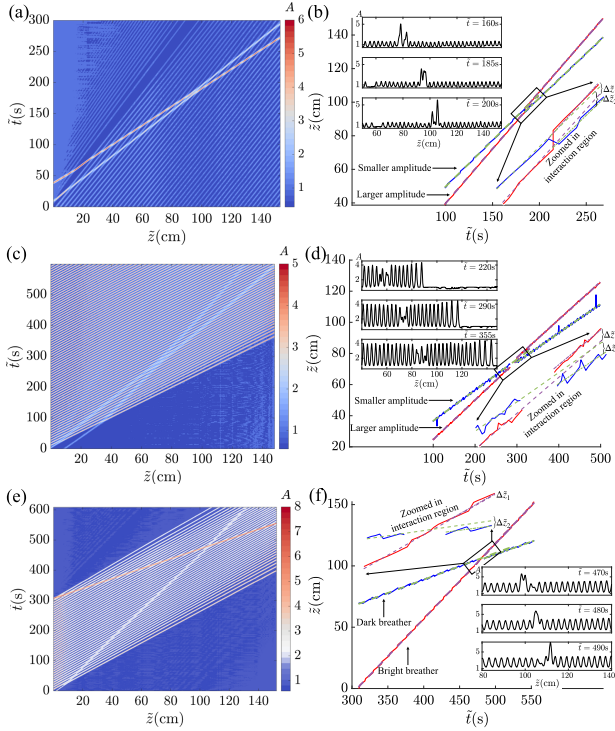


FIG. 4. Observation of traveling breather scattering on a fixed carrier background. (a),(c),(e) Space-time contour revealing conduit dynamics. (b),(d),(f) Traveling breather trajectories (blue and red solid) in the $z-t$ plane with linear fits (dashed) and spatial shifts $\Delta\tilde{z}_j$. Subfigures provide representative spatial profiles at specific times. (a),(b) BB-BB scattering. (c),(d) DB-DB scattering. (e),(f) BB-DB scattering.

[58–60]. For longer times, the simulation and experiment agree very well, demonstrating the stability, robustness, and accuracy of conduit BBs relative to observation. Small carrier discrepancies are due to unphysical periodic boundary conditions and the acknowledged diffusion issues. The DB in Fig. 3(b) has period of oscillation $\tilde{T}_{\text{DB}} = 2\pi/(\tilde{\omega} - \tilde{v}_{\text{DB}}\tilde{k}) \approx 17\text{s}$, depicted in the top four panels. The dimensional timescale T from Eq. (1) used here is 5% smaller than the nominal, measured T extracted from separate linear wave measurements [47]. We attribute this small discrepancy to interior fluid diffusion and limitations of the conduit equation as a model [41]. The KdV DB solution differs from observation, which exhibits a bimodal interaction according to the Lax categories [60]. The DB simulation closely tracks experiment subject to some carrier discrepancies.

The reliable creation of single BBs and DBs in viscous fluid conduits enables the investigation of traveling breather scattering. We create multiple traveling breathers on a fixed carrier background by nonlinear superposing the periodic wave train with two solitons of differing amplitude. Figure 4(a) depicts the scattering of two BBs. The BB created from the larger-amplitude soliton travels at a faster speed and overtakes the smaller amplitude BB. Both BBs are observed to propagate coherently before and after interaction, maintaining essentially the same shape. Figure 4(b) tracks BB peak trajectories. We separately fit the trajectories before and after interaction with linear functions to derive BB speeds \tilde{v}_j and spatial shifts $\Delta\tilde{z}_j$ ($j = 1, 2$) occurring as a result of the interaction (see Table I). For each BB, the speeds pre- and postinteraction are the same, within very small error tolerances, indicating that BB-BB scattering is physically elastic. The faster (slower) BB experiences a positive (negative) spatial shift.

Figure 4(c) presents DB scattering. The larger amplitude DB originating from the larger amplitude soliton moves faster than the smaller amplitude, slower DB. Trajectories in Fig. 4(d) trace the positions of the DB upper envelope minima. Again, DB spatial shifts are observed and DB speeds pre- and postinteraction are conserved (Table I). The faster (slower) DB undergoes a positive (negative) spatial shift.

Since all BBs (DBs) are faster (slower) than the carrier, a BB must overtake a DB for them to interact as shown in Fig. 4(e). The carrier must have finite spatial extent in order to concurrently overtake and be overtaken by a soliton to create a BB and DB. The speed measurements of BB, DB trajectories (Table I) depicted in Fig. 4(f) again indicate that the scattering is physically elastic. The DB spatial shift is negative but the positive BB spatial shift is an order of magnitude smaller, hence the BB is scarcely affected by the DB. In all cases of observed traveling breather scattering, we find that they are physically elastic and faster (slower) traveling breathers experience a positive (negative) spatial shift due to the interaction. This observation is consistent with KdV traveling breather scattering characterized in [30,38].

In Fig. 4, we launch traveling breather pairs on the same carrier background. By considering each traveling breather independently, we can infer their nonlinear dispersion relation. In Fig. 4(a), individual BB phase shifts after interaction are $\Delta\theta_{\text{BB1}} = -1.08\pi$ and $\Delta\theta_{\text{BB2}} = -0.85\pi$.

TABLE I. Speed and spatial shift measurements of traveling breather scattering.

	Traveling breather 1			Traveling breather 2		
	\tilde{v}_1 before (cm/s)	\tilde{v}_1 after (cm/s)	$\Delta\tilde{z}_1$ (cm)	\tilde{v}_2 before (cm/s)	\tilde{v}_2 after (cm/s)	$\Delta\tilde{z}_2$ (cm)
BB-BB	0.65 ± 0.01	0.64 ± 0.01	1.54	0.55 ± 0.01	0.53 ± 0.01	-2.69
DB-DB	0.25 ± 0.01	0.24 ± 0.01	1.75	0.20 ± 0.01	0.19 ± 0.01	-1.97
BB-DB	0.61 ± 0.01	0.62 ± 0.01	0.15	0.22 ± 0.01	0.21 ± 0.01	-1.22

Note that it is standard for a phase shift below $-\pi$ to be shifted to $(0, \pi)$ by adding a 2π period. However, by maintaining the phase shift sign, we can deduce that an increasing BB speed corresponds to an increasing BB amplitude and *decreasing* BB phase shift. This is consistent with the KdV BB dispersion relation [39,47]. In Fig. 4(c), we measure the DB phase shifts postinteraction to be $\Delta\theta_{\text{DB1}} = 0.61\pi$ and $\Delta\theta_{\text{DB2}} = 0.52\pi$. An increasing DB speed corresponds to an increasing DB amplitude and phase shift. For KdV DBs, there are two branches of the DB nonlinear dispersion relation, slow and fast associated with positive and negative phase shifts, respectively [39,47]. Our experimental observations are qualitatively consistent with the nonlinear dispersion relation's slow branch of KdV DBs.

This work experimentally verifies that traveling breathers in a continuum system can be generated from the interaction of solitons and periodic cnoidal-like traveling waves. While continuum traveling breather theory has been developed for integrable systems, our observations and numerical simulations of the two-fluid system suggest that traveling breathers exist in nonintegrable systems as well. Traveling breathers appear to be natural phenomena that occur in continuum environments accompanied by a possibly large-amplitude oscillatory background, distinguishing them from localized breathers. While spectral data analysis techniques have been developed to extract this type of information from complex signals using inverse-scattering-theory-based nonlinear Fourier analysis [61,62], we have physically realized this nonlinear superposition principle with a simple method. The scattering of traveling breathers is observed to be physically elastic (energy conserving) while exhibiting a spatial shift. This work lays the foundation for exploring traveling breathers in other continuum systems such as optics, fluids, condensed matter, and anywhere nonlinear waves occur.

The authors would like to thank the Isaac Newton Institute for Mathematical Sciences, Cambridge, for support and hospitality during the programme *Dispersive hydrodynamics: mathematics, simulation and experiments, with applications in nonlinear waves*, where work on this Letter was discussed. This work was supported by NSF DMS-1816934 and DMS-2306319.

*Corresponding author: yifeng.mao@colorado.edu

- [1] M. J. Ablowitz, D. J. Kaup, A. C. Newell, and H. Segur, Method for Solving the Sine-Gordon Equation, *Phys. Rev. Lett.* **30**, 1262 (1973).
- [2] M. J. Ablowitz and H. Segur, *Solitons and the Inverse Scattering Transform* (SIAM, Philadelphia, 1981).
- [3] A. Kudryavtsev, Solitonlike solutions for a Higgs scalar field, *Pis'ma Zh. Eksp. Teor. Fiz.* **22**, 178 (1975) *JETP Lett.* **22**, 82 (1975).
- [4] M. J. Ablowitz, M. D. Kruskal, and J. Ladik, Solitary wave collisions, *SIAM J. Appl. Math.* **36**, 428 (1979).
- [5] D. K. Campbell, J. F. Schonfeld, and C. A. Wingate, Resonance structure in kink-antikink interactions in ϕ^4 theory, *Physica (Amsterdam)* **9D**, 1 (1983).
- [6] H. Segur and M. D. Kruskal, Nonexistence of Small-Amplitude Breather Solutions in ϕ^4 Theory, *Phys. Rev. Lett.* **58**, 747 (1987).
- [7] A. Soffer and M. I. Weinstein, Resonances, radiation damping and instability in Hamiltonian nonlinear wave equations, *Inventiones Mathematicae* **136**, 9 (1999).
- [8] J. P. Boyd, A numerical calculation of a weakly non-local solitary wave: The ϕ^4 breather, *Nonlinearity* **3**, 177 (1990).
- [9] H. Kalisch, M. A. Alejo, A. J. Corcho, and D. Pilod, Breather solutions to the cubic Whitham equation [arXiv: 2201.12074](https://arxiv.org/abs/2201.12074).
- [10] R. Pethiyagoda, S. W. McCue, and T. J. Moroney, Spectrograms of ship wakes: Identifying linear and nonlinear wave signals, *J. Fluid Mech.* **811**, 189 (2017).
- [11] A. Chabchoub, K. Mozumi, N. Hoffmann, A. V. Babanin, A. Toffoli, J. N. Steer, T. S. van den Bremer, N. Akhmediev, M. Onorato, and T. Waseda, Directional soliton and breather beams, *Proc. Natl. Acad. Sci. U.S.A.* **116**, 9759 (2019).
- [12] R. Grimshaw, J. C. B. da Silva, and J. M. Magalhaes, Modelling and observations of oceanic nonlinear internal wave packets affected by the Earth's rotation, *Ocean Model.* **116**, 146 (2017).
- [13] L. F. Mollenauer, R. H. Stolen, and J. P. Gordon, Experimental Observation of Picosecond Pulse Narrowing and Solitons in Optical Fibers, *Phys. Rev. Lett.* **45**, 1095 (1980).
- [14] D. Mandelik, H. S. Eisenberg, Y. Silberberg, R. Morandotti, and J. S. Aitchison, Observation of Mutually Trapped Multiband Optical Breathers in Waveguide Arrays, *Phys. Rev. Lett.* **90**, 253902 (2003).
- [15] R. W. Boyd, *Nonlinear Optics* (Academic Press, New York, 2013).
- [16] A. Di Carli, C. D. Colquhoun, G. Henderson, S. Flannigan, G.-L. Oppo, A. J. Daley, S. Kuhr, and E. Haller, Excitation Modes of Bright Matter-Wave Solitons, *Phys. Rev. Lett.* **123**, 123602 (2019).
- [17] D. Luo, Y. Jin, J. H. V. Nguyen, B. A. Malomed, O. V. Marchukov, V. A. Yurovsky, V. Dunjko, M. Olshani, and R. G. Hulet, Creation and Characterization of Matter-Wave Breathers, *Phys. Rev. Lett.* **125**, 183902 (2020).
- [18] C. Kharif, E. N. Pelinovsky, and A. Slunyaev, *Rogue Waves in the Ocean*, Advances in Geophysical and Environmental Mechanics and Mathematics (Springer, Berlin, 2009).
- [19] B. Kibler, J. Fatome, C. Finot, G. Millot, F. Dias, G. Genty, N. Akhmediev, and J. M. Dudley, The Peregrine soliton in nonlinear fibre optics, *Nat. Phys.* **6**, 790 (2010).
- [20] A. Chabchoub, N. P. Hoffmann, and N. Akhmediev, Rogue Wave Observation in a Water Wave Tank, *Phys. Rev. Lett.* **106**, 204502 (2011).
- [21] M. N arhi, B. Wetzel, C. Billet, S. Toenger, T. Sylvestre, J.-M. Merolla, R. Morandotti, F. Dias, G. Genty, and J. M. Dudley, Real-time measurements of spontaneous breathers and rogue wave events in optical fibre modulation instability, *Nat. Commun.* **7**, 13675 (2016).
- [22] A. Tikan, F. Bonnefoy, G. Roberti, G. El, A. Tovbis, G. Ducrozet, A. Cazaubiel, G. Prabhudesai, G. Michel,

- F. Copie, E. Falcon, S. Randoux, and P. Suret, Prediction and manipulation of hydrodynamic rogue waves via nonlinear spectral engineering, *Phys. Rev. Fluids* **7**, 054401 (2022).
- [23] M. Wu, Nonlinear spin waves in magnetic film feedback rings, *Solid State Phys.* **62**, 163 (2010).
- [24] S. Flach and A. V. Gorbach, Discrete breathers—Advances in theory and applications, *Phys. Rep.* **467**, 1 (2008).
- [25] N. Boechler, G. Theocharis, S. Job, P. G. Kevrekidis, M. A. Porter, and C. Daraio, Discrete Breathers in One-Dimensional Diatomic Granular Crystals, *Phys. Rev. Lett.* **104**, 244302 (2010).
- [26] G. Iooss and G. James, Localized waves in nonlinear oscillator chains, *Chaos* **15**, 015113 (2005).
- [27] G. James, Travelling breathers and solitary waves in strongly nonlinear lattices, *Phil. Trans. R. Soc. A* **376**, 20170138 (2018).
- [28] M. Sato and A. J. Sievers, Driven Localized Excitations in the Acoustic Spectrum of Small Nonlinear Macroscopic and Microscopic Lattices, *Phys. Rev. Lett.* **98**, 214101 (2007).
- [29] E. Kim, F. Li, C. Chong, G. Theocharis, J. Yang, and P. G. Kevrekidis, Highly Nonlinear Wave Propagation in Elastic Woodpile Periodic Structures, *Phys. Rev. Lett.* **114**, 118002 (2015).
- [30] E. A. Kuznetsov and A. V. Mikhailov, Stability of stationary waves in nonlinear weakly dispersive media, *Zh. Eksp. Teor. Fiz.* **67**, 1717 (1974) [*Sov. Phys. JETP* **40**, 855 (1975)], <https://ui.adsabs.harvard.edu/abs/1975JETP..40..855K>.
- [31] E. D. Belokolos, A. I. Bobenko, V. Z. Enolski, A. R. Its, and V. B. Matveev, *Algebro-Geometric Approach to Nonlinear Integrable Equations* (Springer, New York, 1994).
- [32] F. Gesztesy and R. Svirsky, *M-KdV Solitons on the Background of Quasi-Periodic Finite-Gap Solutions* (American Mathematical Society, Providence, USA, 1995).
- [33] X.-R. Hu, S.-Y. Lou, and Y. Chen, Explicit solutions from eigenfunction symmetry of the Korteweg–de Vries equation, *Phys. Rev. E* **85**, 056607 (2012).
- [34] S. Lou, Consistent riccati expansion for integrable systems, *Stud. Appl. Math.* **134**, 372 (2015).
- [35] D. A. Takahashi, Integrable model for density-modulated quantum condensates: Solitons passing through a soliton lattice, *Phys. Rev. E* **93**, 062224 (2016).
- [36] E. A. Kuznetsov, Fermi–Pasta–Ulam recurrence and modulation instability, *JETP Lett.* **105**, 125 (2017).
- [37] A. Nakayashiki, One step degeneration of trigonal curves and mixing of solitons and quasi-periodic solutions of the KP equation, in *Geom. Methods Phys. XXXVIII*, Trends in Mathematics, edited by P. Kielanowski, A. Odziejewicz, and E. Previato (Springer International Publishing, Cham, 2020), pp. 163–186.
- [38] M. Bertola, R. Jenkins, and A. Tovbis, Partial degeneration of finite gap solutions to the Korteweg-de Vries equation: Soliton gas and scattering on elliptic background, *Nonlinearity* **36**, 3622 (2023).
- [39] M. A. Hoefer, A. Mucalica, and D. E. Pelinovsky, Kdv breathers on a cnoidal background, *J. Phys. A: Math. Theor.* **56**, 185701 (2023).
- [40] I. M. Krichever, Potentials with zero coefficient of reflection on a background of finite-zone potentials, *Funct. Anal. Appl.* **9**, 161 (1975).
- [41] Y. Mao and M. A. Hoefer, Experimental investigations of linear and nonlinear periodic travelling waves in a viscous fluid conduit, *J. Fluid Mech.* **954**, A14 (2023).
- [42] M. d'OLCE, J. Martin, N. Rakotomalala, D. Salin, and L. Talon *et al.*, Convective/absolute instability in miscible core-annular flow. Part 1: Experiments, *J. Fluid Mech.* **618**, 305 (2009).
- [43] B. Selvam, L. Talon, L. Lesshafft, and E. Meiburg, Convective/absolute instability in miscible core-annular flow. Part 2. Numerical simulations and nonlinear global modes, *J. Fluid Mech.* **618**, 323 (2009).
- [44] D. R. Scott, D. J. Stevenson, and J. A. Whitehead, Observations of solitary waves in a viscously deformable pipe, *Nature (London)* **319**, 759 (1986).
- [45] P. Olson and U. Christensen, Solitary wave propagation in a fluid conduit within a viscous matrix, *J. Geophys. Res.* **91**, 6367 (1986).
- [46] N. K. Lowman and M. A. Hoefer, Dispersive hydrodynamics in viscous fluid conduits, *Phys. Rev. E* **88**, 023016 (2013).
- [47] See Supplemental Material at <http://link.aps.org/supplemental/10.1103/PhysRevLett.131.147201> for additional mathematical and experimental details, which includes Ref. [48].
- [48] J. A. Whitehead Jr. and D. S. Luther, Dynamics of laboratory diapir and plume models, *J. Geophys. Res.* **80**, 705 (1975).
- [49] V. Barcion and F. M. Richter, Nonlinear waves in compacting media, *J. Fluid Mech.* **164**, 429 (1986).
- [50] A. G. Stubblefield, M. Spiegelman, and T. T. Creyts, Solitary waves in power-law deformable conduits with laminar or turbulent fluid flow, *J. Fluid Mech.* **886**, A10 (2020).
- [51] S. E. Harris, P. A. Clarkson *et al.*, Painlevé analysis and similarity reductions for the magma equation, *SIGMA* **2**, 068 (2006).
- [52] M. D. Maiden and M. A. Hoefer, Modulations of viscous fluid conduit periodic waves, *Proc. R. Soc. A* **472**, 20160533 (2016).
- [53] K. R. Helfrich and J. A. Whitehead, Solitary waves on conduits of buoyant fluid in a more viscous fluid, *Geophys. Astrophys. Fluid Dyn.* **51**, 35 (1990).
- [54] M. D. Maiden, N. K. Lowman, D. V. Anderson, M. E. Schubert, and M. A. Hoefer, Observation of Dispersive Shock Waves, Solitons, and Their Interactions in Viscous Fluid Conduits, *Phys. Rev. Lett.* **116**, 174501 (2016).
- [55] S. Gavriluk and K.-M. Shyue, Singular solutions of the BBM equation: Analytical and numerical study, *Nonlinearity* **35**, 388 (2021).
- [56] M. D. Maiden, D. V. Anderson, N. A. Franco, G. A. El, and M. A. Hoefer, Solitonic Dispersive Hydrodynamics: Theory and Observation, *Phys. Rev. Lett.* **120**, 144101 (2018).
- [57] G. B. Whitham, Comments on periodic waves and solitons, *IMA J. Appl. Math.* **32**, 353 (1984).

- [58] P.D. Lax, Integrals of nonlinear equations of evolution and solitary waves, *Commun. Pure Appl. Math.* **21**, 467 (1968).
- [59] W. Craig, P. Guyenne, J. Hammack, D. Henderson, and C. Sulem, Solitary water wave interactions, *Phys. Fluids* **18**, 057106 (2006).
- [60] N. K. Lowman, M. A. Hoefer, and G. A. El, Interactions of large amplitude solitary waves in viscous fluid conduits, *J. Fluid Mech.* **750**, 372 (2014).
- [61] A. Costa, A. R. Osborne, D. T. Resio, S. Alessio, E. Chrivì, E. Saggese, K. Bellomo, and C. E. Long, Soliton Turbulence in Shallow Water Ocean Surface Waves, *Phys. Rev. Lett.* **113**, 108501 (2014).
- [62] M. Brühl, P. J. Prins, S. Ujvary, I. Barranco, S. Wahls, and P. L. F. Liu, Comparative analysis of bore propagation over long distances using conventional linear and KdV-based nonlinear Fourier transform, *Wave Motion* **111**, 102905 (2022).